Physics Letters B 764 (2017) 42–48

Contents lists available at ScienceDirect

Physics Letters B

www.elsevier.com/locate/physletb

Ways to produce new superheavy isotopes with $Z = 111$–117 in charged particle evaporation channels

Juhee Hong [a], G.G. Adamian [b,*], N.V. Antonenko [b,c]

[a] Rare Isotope Science Project, Institute for Basic Science, Daejeon 34047, Republic of Korea
[b] Joint Institute for Nuclear Research, Dubna 141980, Russia
[c] Mathematical Physics Department, Tomsk Polytechnic University, 634050 Tomsk, Russia

ARTICLE INFO

Article history:
Received 27 September 2016
Received in revised form 1 November 2016
Accepted 3 November 2016
Available online 9 November 2016
Editor: V. Metag

Keywords:
Superheavy nuclei
Complete fusion reactions
Production of new isotopes
Charged particle evaporation channels

ABSTRACT

The excitation functions of the production of new heaviest isotopes of superheavy nuclei with charge numbers 111–117 in the *pxn* and *αxn* evaporation channels of the ^{48}Ca-induced hot fusion reactions are predicted for the first time for future experiments.

1. Introduction

The ^{48}Ca-induced actinide-based complete fusion reactions have been intensively and successfully used to produce superheavy nuclei (SHN) with the charge numbers $Z = 112$–118 in the neutron-evaporation channels (*xn*-channels) [1–11] and to approach to "the island of stability" of SHN predicted at $Z = 114$–126 and neutron numbers $N = 172$–184 by the nuclear shell models [12–14]. The further experimental extension of the region of SHN in the direction of the magic neutron number $N = 184$, the center of the predicted "island of stability", in the *xn*-channels is limited by the number of available stable projectiles and targets and the small production cross sections. Because the intensive radioactive beams are not available so far, new isotopes of heaviest nuclei with $Z = 111$–117 can be synthesized in the ^{48}Ca-induced actinide-based complete fusion-evaporation reactions with the emission of charged particles from the compound nucleus (CN). The evaporation of proton or alpha-particle from CN in these reactions leads to the formation of nuclei with smaller Z, but with larger neutron excess. In addition, in the nucleus formed the electron capture can occur by converting a proton into a neutron to the daughter nucleus. Note that the possibility of the production of new heaviest isotopes of superheavy nuclei with charge numbers 113, 115, and 117 in the proton evaporation channels with rather high efficiency was suggested for the first time in Ref. [15]. In the present article we focus on the possibility of the direct production of heaviest isotopes with $111 \leq Z \leq 117$ in the *pxn* and *αxn* evaporation channels.

2. Model

For the excited SHN, the emission of charged particles is suppressed by the high Coulomb barrier and competes with the neutron evaporation and fission. The evaporation residue cross section [16–29]

$$\sigma_s(E_{\mathrm{c.m.}}) = \sum_J \sigma_{cap}(E_{\mathrm{c.m.}}, J) P_{CN}(E_{\mathrm{c.m.}}, J) W_s(E_{\mathrm{c.m.}}, J) \qquad (1)$$

in the evaporation channel s depends on the partial capture cross section σ_{cap} for the transition of the colliding nuclei over the entrance (Coulomb) barrier, the probability of CN formation P_{CN} after the capture and the survival probability W_s of the excited CN. The formation of CN is described within a version of the dinuclear system model [28,29]. In the first step of a fusion reaction the projectile is captured by the target. In the second step a formed dinuclear system (DNS) evolves into the CN in the mass asymmetry coordinate $\eta = (A_1 - A_2)/(A_1 + A_2)$ (A_1 and A_2 are the mass numbers

* Corresponding author.
E-mail address: adamian@theor.jinr.ru (G.G. Adamian).

http://dx.doi.org/10.1016/j.physletb.2016.11.002

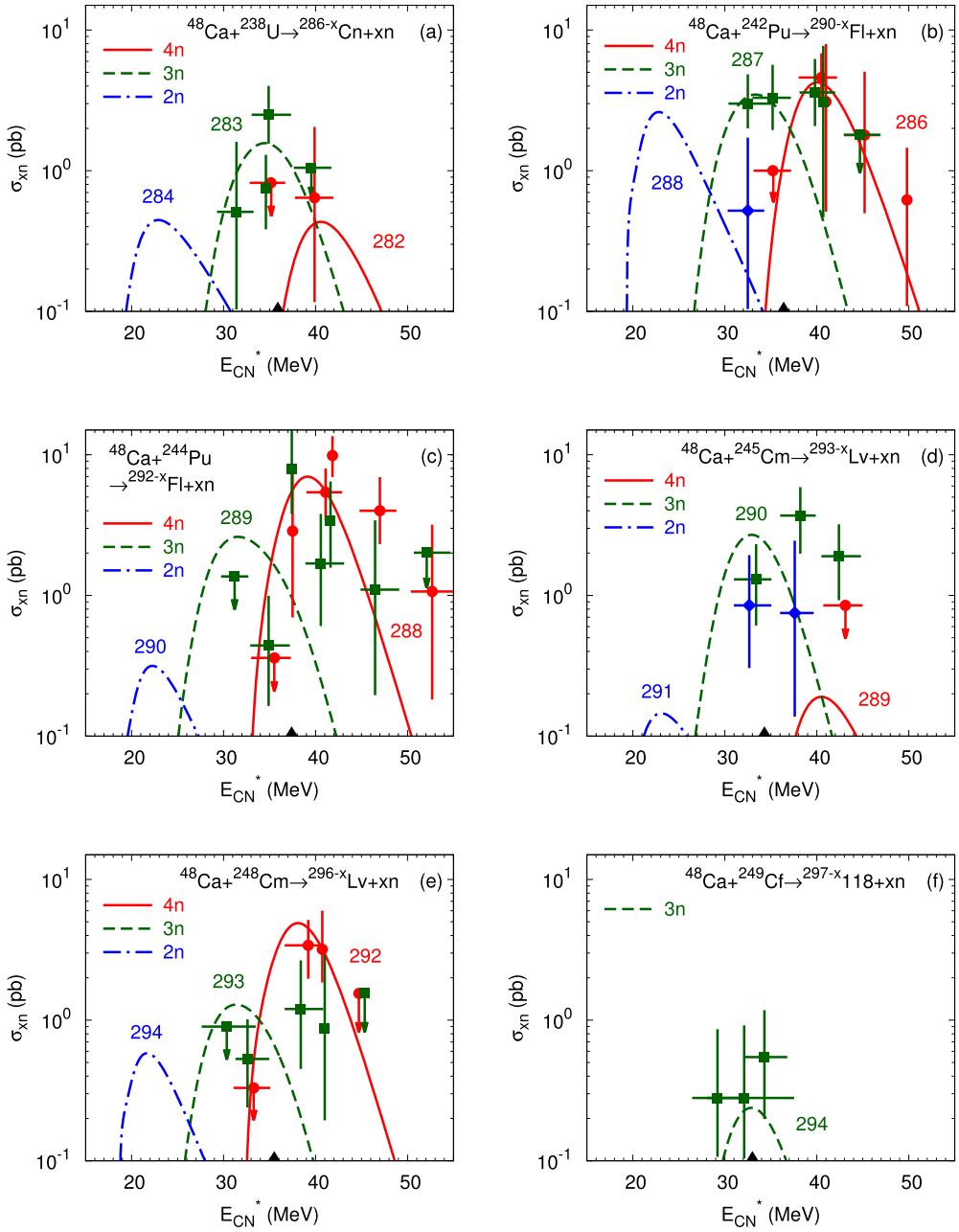

Fig. 1. (Color online.) The measured (symbols) and calculated (lines) excitation functions for xn evaporation channels of the indicated complete fusion reactions. The mass table of Ref. [38] is used in the calculations. The mass numbers of isotopes produced are indicated. The black triangles at the energy axis indicate the excitation energy $E^*_{CN} = V_b + Q$ of the CN at bombarding energy corresponding to the Coulomb barrier V_b ($E_{\text{c.m.}} = V_b$). The blue diamonds, green squares, and red circles represent the experimental data [3] with error bars for $2n$, $3n$, and $4n$ evaporation channels, respectively. The horizontal line with arrow is the upper limit of the evaporation residue cross sections in given xn-channel.

of the DNS nuclei) [16–24,26,27,29]. Since the bombarding energy $E_{\text{c.m.}}$ of the projectile is usually higher than the Q value for the CN formation, the produced nucleus is excited. In the third step of the reaction the CN loses its excitation energy mainly by the emission of particles and γ-quanta [30–37]. In the de-excitation of a CN, the charged particle emission competes with the fission and neutron emission. We describe the production of nuclei in the evaporation channels with emission of charged particle (proton or α-particle) and neutrons as in Ref. [29]. The emissions of γ, deuteron, triton, and clusters heavier than alpha-particle are assumed to be negligible to contribute to the total width of the CN decay. The de-excitation of the CN is treated with the statistical model using the level densities from the Fermi-gas model. The neutron B_n, proton B_p, and alpha-particle B_α binding energies, the nuclear mass excesses of superheavy nuclei, and the ground-state microscopic corrections (their absolute values are approximately equal to the fission barriers for the nuclei considered) are taken from Ref. [38]. With the level density parameter $a_n = a = A/10$ MeV^{-1} for neutron (A is the mass number of the CN), the level density parameters for fission, proton-emission, and α-emission channels are taken as $a_f = 1.03a$, $a_p = 0.96a$, and $a_\alpha = 1.15a$, respectively. For the calculation of the Coulomb barrier, we use the expression

$$V_j = \frac{(Z - z_j)z_j e^2}{r_j[(A - m_j)^{1/3} + m_j^{1/3}]}, \tag{2}$$

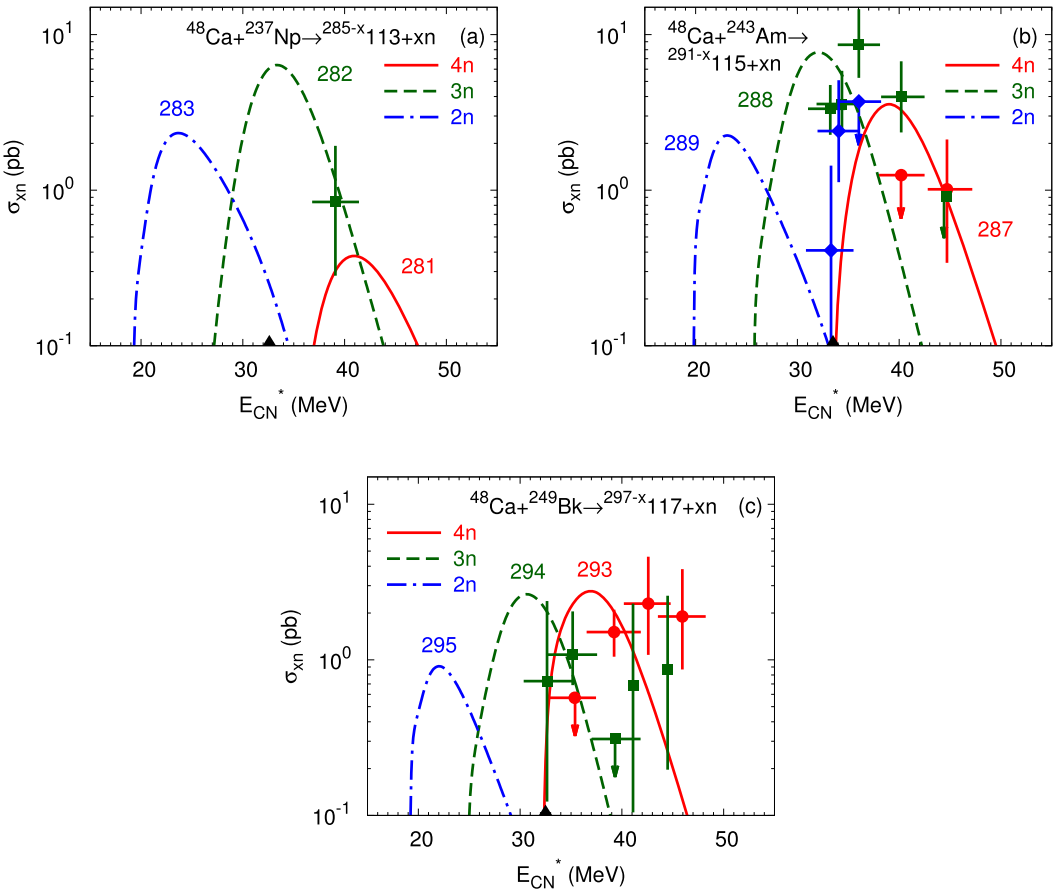

Fig. 2. (Color online.) The same as in Fig. 1, but for other indicated complete fusion reactions.

where z_j (m_j) are the charge (mass) numbers of the charged particle (proton or α-particle) and r_j is a constant. The charge Z (mass A) number corresponds to the CN. There are different theoretical estimations of r_j [30,37]. In the case of α emission, r_α varies from 1.3 to 1.78 fm. We obtain r_α from the energy of the DNS formed by the daughter nucleus and α-particle. We calculate the Coulomb barrier in the interaction potential between the α-particle and the daughter nucleus [39], and find the value of r_α from Eq. (2). For different nuclei considered, we obtained $r_\alpha = 1.57$ fm using this method. Thus, in the calculations of V_α we set $r_\alpha = 1.57$ fm for nuclei considered. The parameter r_p for the Coulomb barrier for proton emission is taken as $r_p = 1.7$ fm from Refs. [26,37]. As seen, the values of σ_s near the maximum are almost insensitive to the variations of this parameter, but far from the maximum they change up to one order of magnitude. We would like to stress the weak dependence of the calculated σ_s near the maxima of the excitation functions on the reasonable variation of all parameters discussed. Therefore, the results obtained in this paper have quite a small uncertainty near the maxima of the excitation functions which are important for the maximum yield of a certain nucleus in the experiments. We estimate this uncertainty within a factor of 2–4. Our calculations are tested for many known reactions in which the excitation functions of transfermium nuclei produced in the charged particle evaporation channels have been measured [29].

3. Calculated results

The fusion model discussed above is used to calculate the excitation functions of the actinide-based hot fusion reactions and compare them with the available experimental data. In Figs. 1 and 2, the experimental cross sections of the xn evaporation channels are compared with the calculated evaporation residue cross sections. The calculated results agree well with most of the data. The disagreements in some cases (for example, in the $2n$-channel) should be considered in light of the absence of special fit with the parameters used and the theoretical and experimental uncertainties, especially at sub-barrier energies and at energies far from the maximum of the excitation function.

As seen in Figs. 3–5, and Table 1 the unknown heaviest isotopes ^{283,284}Rg, ^{287,288}113, $^{288-290}$113 (^{286,287}Cn), ^{291}115, $^{292-294}$115 (^{290,291}Fl), ^{295}117, and $^{295-297}$117 (^{294}Lv) can be produced in the pxn-channels (αxn-channels) of the reactions ^{48}Ca + ^{238}U, ^{48}Ca+^{242}Pu, ^{48}Ca+^{244}Pu, ^{48}Ca+^{245}Cm, ^{48}Ca+^{248}Cm, ^{48}Ca+^{249}Cf, and ^{48}Ca + ^{251}Cf, respectively. Because $B_p + V_p > B_\alpha + V_\alpha$ (Table 2), the production cross sections in the pxn-channels are smaller than those in the αxn evaporation channels. In all reactions, except ^{48}Ca + ^{249}Cf where $\sigma_{p1n} \approx \sigma_{p2n}$, the optimal proton evaporation channel is the $p2n$-channel. The optimal alpha-emission channel is $\alpha 2n$ or $\alpha 1n$. The interval of maximum production cross section is about (1–60) fb in the pxn-channels and (3–600) fb in the αxn-channels. For example, in the pxn-channels (αxn-channels) of the reactions ^{48}Ca + ^{244}Pu, ^{48}Ca + ^{248}Cm, and ^{48}Ca+^{251}Cf, the evaporation residue cross sections of nuclei ^{289}113 (^{286}Cn), ^{293}115 (^{290}Fl), and ^{296}117 (^{294}Lv) are 27 fb (43 fb), 59 fb (610 fb), and 16 fb (220 fb), respectively (Table 1). The cross sections in the ^{48}Ca + ^{248}Cm reaction are larger than those in the reactions ^{48}Ca + ^{244}Pu and ^{48}Ca + ^{251}Cf because after the charged particle emission the daughter nuclei produced in the ^{48}Ca+^{248}Cm reaction have larger fission barriers and $B_f - B_n$, and, correspond-

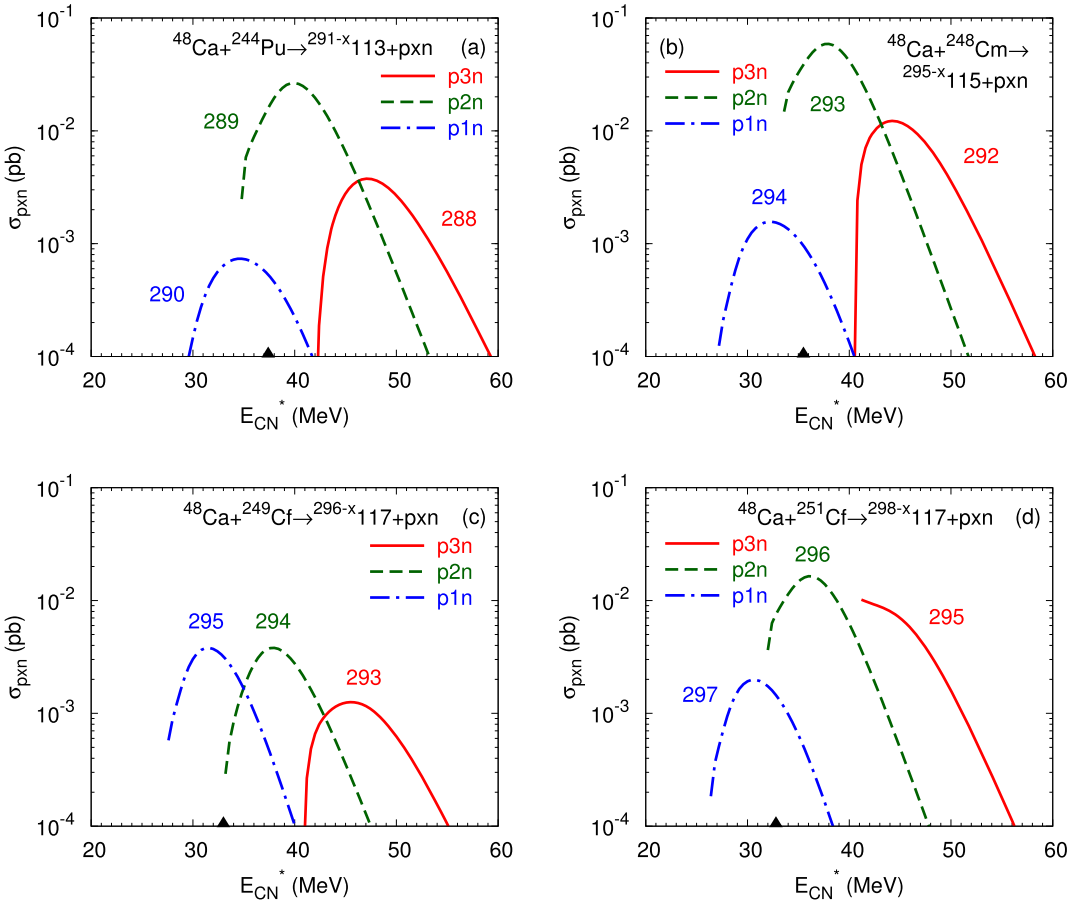

Fig. 3. (Color online.) The calculated (lines) excitation functions for pxn evaporation channels of the indicated complete fusion reactions. There is energy cutting of the left-hand side of the excitation function. The mass table of Ref. [38] is used in the calculations. The mass numbers of isotopes produced are indicated. The black triangles at the energy axis indicate the excitation energy $E^*_{CN} = V_b + Q$ of the CN at bombarding energy corresponding to the Coulomb barrier V_b ($E_{\text{c.m.}} = V_b$).

ingly, larger probability of neutron emission. For the reactions considered, the value of $B_i + V_i$ ($i = p, \alpha$) globally decreases with increasing Z of CN (Table 2). The value of $B_f - B_n$ has maxima for the CN with $Z = 115$ and 114. As a result, the production cross sections in the pxn and αxn evaporation channels are maximum in the ^{48}Ca + ^{248}Cm reaction leading to the CN with $Z = 116$.

The maximum production cross sections of the known isotopes $^{278-280}$Rg and $^{284-286}$113 in the αxn-channels of the reactions ^{48}Ca + ^{237}Np and ^{48}Ca + ^{243}Am are about 8, 23, 37 fb and 36, 240, 49 fb, respectively. As seen in Table 1 and Fig. 5, the unknown heaviest isotope(s) ^{294}Lv (^{291,292}115) can be produced in the $p2n$-channel ($\alpha 2n$-, $\alpha 1n$-channels) of the ^{48}Ca+^{249}Bk reaction. In contrast to the reactions with odd-Z targets, one can produce more neutron-rich isotopes in the reactions with even-Z targets.

Since the known heaviest isotopes are ^{286}113, ^{290}115, and ^{294}117 (^{285}Cn, ^{289}Fl, and ^{293}Lv), the use of the charged particle evaporation channels allows us to increase the mass number of heaviest isotopes by 4, 4, and 3 (2, 2, and 1) units, respectively. Note that the proton evaporation channels are more effective to approach $N = 184$ than the alpha emission channels.

In the proton emission channels, the evaporation residue cross sections are usually smaller than those in the neutron evaporation channels (Figs. 1–4) because of the larger proton binding plus Coulomb barrier energy ($B_p + V_p > B_n$) (Table 2). In the ^{48}Ca + ^{244}Pu (^{48}Ca + ^{248}Cm) reaction, the maximum cross section of the $p2n$ evaporation channel is about 96 (22) times smaller than that of the $3n$ emission channel. In the reactions ^{48}Ca + ^{249}Cf and ^{48}Ca + ^{251}Cf the ratios σ_{3n}/σ_{p2n} are 63 and 37, respectively (Table 1). The results of calculations show that even the $2n$-channel, which is at energies under the Coulomb barrier, is more favorable for producing some new isotopes than the corresponding pxn-channel. For instance, in the production of the nuclei ^{289}115, ^{294}Lv, and ^{295}117 we obtain $\sigma_{2n}(^{48}\text{Ca} + {}^{243}\text{Am}) > \sigma_{p3n}(^{48}\text{Ca} + {}^{245}\text{Cm})$, $\sigma_{2n}(^{48}\text{Ca} + {}^{248}\text{Cm}) > \sigma_{p2n}(^{48}\text{Ca} + {}^{249}\text{Bk})$, and $\sigma_{2n}(^{48}\text{Ca} + {}^{249}\text{Bk}) > \sigma_{p1n}(^{48}\text{Ca} + {}^{249}\text{Cf})$, $\sigma_{2n}(^{48}\text{Ca} + {}^{249}\text{Bk}) > \sigma_{p3n}(^{48}\text{Ca} + {}^{251}\text{Cf})$, respectively (Table 1). Because the increase of the survival probability with increasing neutron number is almost compensated by the decrease of the fusion probability, $\sigma_{p2n}(^{48}\text{Ca} + {}^{242}\text{Pu}) \approx \sigma_{p2n}(^{48}\text{Ca} + {}^{244}\text{Pu})$, $\sigma_{p3n}(^{48}\text{Ca} + {}^{242}\text{Pu}) \approx \sigma_{p3n}(^{48}\text{Ca} + {}^{244}\text{Pu})$.

As seen in Figs. 1, 2, and 5, $\sigma_{xn} > \sigma_{\alpha yn}$ ($x = 2-4$ and $y = 1-3$) and the formation of new isotopes in the (HI, αyn)-reactions occurs with higher cross sections than those in the (HI, pyn)-reactions. For example, in the reactions ^{48}Ca + ^{238}U, ^{48}Ca + ^{244}Pu, and ^{48}Ca + ^{251}Cf we obtain $\sigma_{3n}/\sigma_{\alpha 2n} \approx 160$, 60, and 3, respectively. In the ^{48}Ca + ^{248}Cm reaction, we get $\sigma_{3n}/\sigma_{\alpha 2n} \approx 2$ and $\sigma_{2n}/\sigma_{\alpha 2n} \approx 1$ (Table 1). These small ratios are probably due to the low energy threshold $B_\alpha + V_\alpha$ and large value of $P_{\alpha 2n}$ for this reaction. Moreover the predicted fission barriers of the daughter nuclei Fl formed after the α-emission are rather high in Ref. [38]. One can also observe in Figs. 1, 2, 5, and Table 1 that $\sigma_{3n}(^{48}\text{Ca} + {}^{248}\text{Cm}) > \sigma_{\alpha 2n}(^{48}\text{Ca} + {}^{251}\text{Cf})$, $\sigma_{2n}(^{48}\text{Ca} + {}^{248}\text{Cm}) > \sigma_{\alpha 1n}(^{48}\text{Ca} + {}^{251}\text{Cf})$ in the production of the nuclei ^{293,294}Lv, respectively.

The predicted cross sections are almost independent within the factor of 1–3 on the choice of the macroscopic-microscopic mass table based on the magic number $Z = 114$. This variation is almost within the inaccuracy of present calculation.

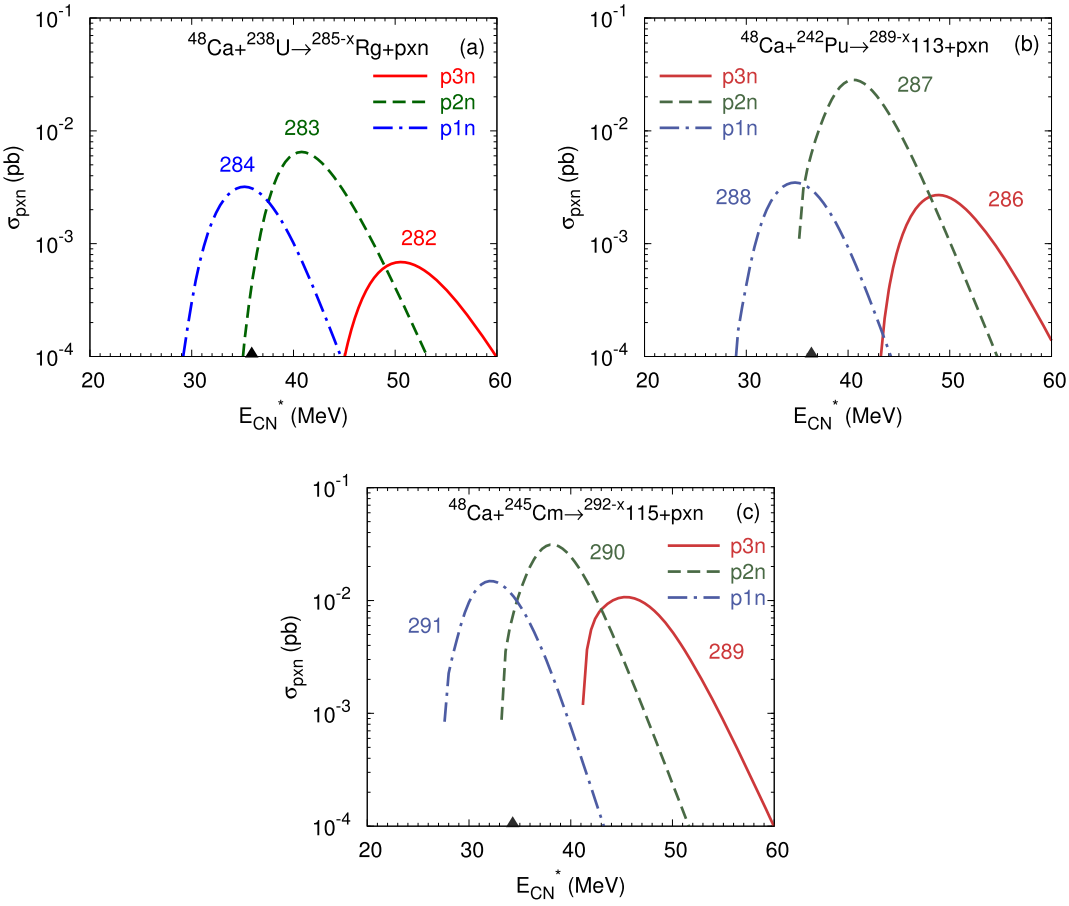

Fig. 4. (Color online.) The same as in Fig. 3, but for other indicated complete fusion reactions.

Table 1
The calculated maximum production cross sections of new isotopes in pxn and αxn evaporation channels of the indicated complete fusion reactions. The mass table of Ref. [38] is used in the calculations.

Reaction	E^*_{CN} (MeV)	σ_s (fb)
$^{48}Ca + ^{238}U \to ^{284}Rg + p1n$	35	3
$^{48}Ca + ^{238}U \to ^{283}Rg + p2n$	41	7
$^{48}Ca + ^{242}Pu \to ^{288}113 + p1n$	35	4
$^{48}Ca + ^{242}Pu \to ^{287}113 + p2n$	40	28
$^{48}Ca + ^{244}Pu \to ^{290}113 + p1n$	35	0.7
$^{48}Ca + ^{244}Pu \to ^{289}113 + p2n$	40	27
$^{48}Ca + ^{244}Pu \to ^{288}113 + p3n$	47	4
$^{48}Ca + ^{244}Pu \to ^{287}Cn + \alpha 1n$	37	3
$^{48}Ca + ^{244}Pu \to ^{286}Cn + \alpha 2n$	43	43
$^{48}Ca + ^{245}Cm \to ^{291}115 + p1n$	32	15
$^{48}Ca + ^{248}Cm \to ^{294}115 + p1n$	32	2
$^{48}Ca + ^{248}Cm \to ^{293}115 + p2n$	38	59
$^{48}Ca + ^{248}Cm \to ^{292}115 + p3n$	44	12
$^{48}Ca + ^{248}Cm \to ^{291}Fl + \alpha 1n$	34	29
$^{48}Ca + ^{248}Cm \to ^{290}Fl + \alpha 2n$	39	610
$^{48}Ca + ^{249}Bk \to ^{294}Lv + p2n$	37	5
$^{48}Ca + ^{249}Bk \to ^{292}115 + \alpha 1n$	32	45
$^{48}Ca + ^{249}Bk \to ^{291}115 + \alpha 2n$	37	900
$^{48}Ca + ^{249}Cf \to ^{295}117 + p1n$	32	4
$^{48}Ca + ^{251}Cf \to ^{297}117 + p1n$	31	2
$^{48}Ca + ^{251}Cf \to ^{296}117 + p2n$	36	16
$^{48}Ca + ^{251}Cf \to ^{295}117 + p3n$	41	10
$^{48}Ca + ^{251}Cf \to ^{294}Lv + \alpha 1n$	31	88

Table 2
The calculated proton and alpha-particle barriers V_i ($i = p, \alpha$), and the proton and alpha-particle binding energies B_i from Ref. [38].

Reaction	V_p (MeV)	V_α (MeV)	$B_p + V_p$ (MeV)	$B_\alpha + V_\alpha$ (MeV)
$^{48}Ca + ^{238}U$	12.4	24.8	16.9	16.3
$^{48}Ca + ^{242}Pu$	12.6	25.1	17.1	16.6
$^{48}Ca + ^{244}Pu$	12.6	25.1	17.2	16.9
$^{48}Ca + ^{245}Cm$	12.8	25.5	15.5	14.6
$^{48}Ca + ^{248}Cm$	12.7	25.5	15.9	14.4
$^{48}Ca + ^{249}Cf$	12.9	25.9	14.8	13.8
$^{48}Ca + ^{251}Cf$	12.9	25.9	15.1	13.3

4. Conclusions

The production cross sections of heaviest unknown isotopes ^{283,284}Rg, $^{287-290}$113, $^{291-294}$115, ^{294}Lv, and $^{295-297}$117 (^{286,287}Cn, ^{290,291}Fl, ^{291,292}115, and ^{294}Lv) in the pxn-channels (αxn-channels) of the ^{48}Ca-induced hot fusion reactions were predicted for the first time: about (1–60) fb in the pxn-channels ((3–900) fb in the αxn-channels). The use of the charged particle evaporation channels allows us to increase the mass number of heaviest isotopes of nuclei with $Z = 111$, 113, 115, and 117 (112, 114, and 116) by 2, 4, 4, and 3 (2, 2, and 1) units, respectively. In addition, in the nuclei produced the electron capture can occur by adding one more neutron in the daughter nuclei. The proton evaporation channels are more effective to approach $N = 184$ than the alpha emission channels. One can produce more neutron-rich isotopes in the reactions with even-Z targets than in the reactions with odd-Z ones. Although the production of some isotopes in $2n$ evaporation channels is more favorable, the pxn and αxn evaporation channels

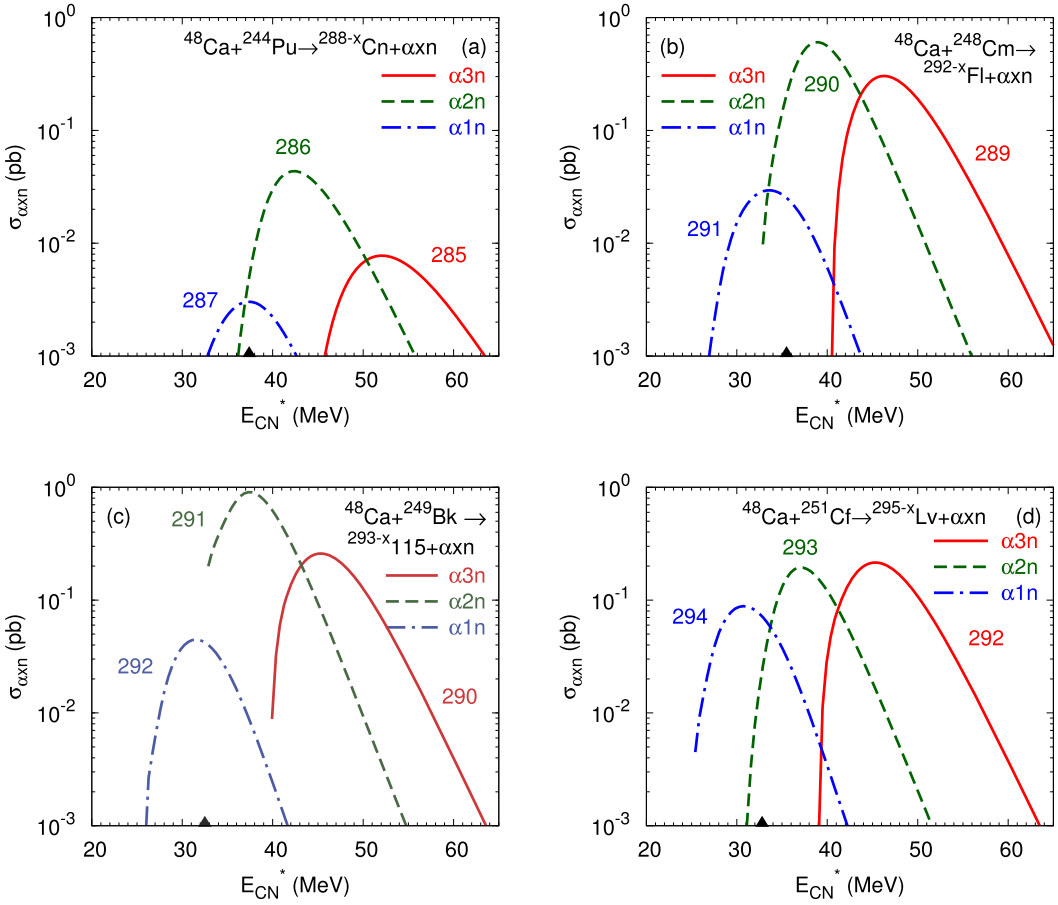

Fig. 5. (Color online.) The calculated (lines) excitation functions for αxn evaporation channels of the indicated complete fusion reactions. The mass table of Ref. [38] is used in the calculations. The mass numbers of isotopes produced are indicated. The black triangles at the energy axis indicate the excitation energy $E^*_{CN} = V_b + Q$ of the CN at bombarding energy corresponding to the Coulomb barrier V_b ($E_{\text{c.m.}} = V_b$).

allows us to obtain an access to those isotopes which are unreachable in the xn-channels due to the lack of proper projectile-target combination. Thus, employing reactions suggested, one can produce unknown heaviest isotopes closer to the center of the island of stability. The pxn- and αxn-channels can be only distinguished by different α-decay chains of the evaporation residues because the excitation functions of these channels overlap with those from xn-channels. All production cross sections in the charged particle evaporation channels are smaller than in the xn-channels.

Acknowledgements

We are thankful to Prof. Yu.Ts. Oganessian for the initialization of this work and many fruitful discussions. We thank Prof. S. Hofmann, Prof. Y. Kim, and Prof. H. Lenske for useful and interesting discussions. This work is supported by the Rare Isotope Science Project of Institute for Basic Science funded by Ministry of Science, ICT and Future Planning and National Research Foundation of Korea (2013M7A1A1075764). G.G.A. and N.V.A. acknowledge the partial supports from the Alexander von Humboldt-Stiftung (Bonn), DFG (Bonn), and the Russian Foundation for Basic Research (Moscow).

References

[1] Yu.Ts. Oganessian, J. Phys. G 34 (2007) R165.
[2] Yu.Ts. Oganessian, et al., Phys. Rev. Lett. 104 (2010) 142502;
Phys. Rev. C 87 (2013) 014302;
Phys. Rev. C 87 (2013) 034605;
Phys. Rev. C 87 (2013) 054621;
V.K. Utyonkov, et al., Phys. Rev. C 92 (2015) 034609.
[3] Yu.Ts. Oganessian, V.K. Utyonkov, Nucl. Phys. A 944 (2015) 62.
[4] R. Eichler, et al., Nature 447 (2007) 72.
[5] S. Hofmann, et al., Eur. Phys. J. A 32 (2007) 251.
[6] L. Stavsetra, K.E. Gregorich, J. Dvorak, P.A. Ellison, I. Dragojevic, M.A. Garcia, H. Nitsche, Phys. Rev. Lett. 103 (2009) 132502.
[7] Ch. Düllmann, et al., Phys. Rev. Lett. 104 (2010) 252701.
[8] J.M. Gates, et al., Phys. Rev. C 83 (2011) 054618.
[9] S. Hofmann, et al., Eur. Phys. J. A 48 (2012) 62.
[10] J.M. Khuyagbaatar, et al., Phys. Rev. Lett. 112 (2014) 172501.
[11] S. Hofmann, et al., Eur. Phys. J. A 52 (2016) 180.
[12] A. Sobiczewski, F.A. Gareev, B.N. Kalinkin, Phys. Lett. B 2 (1966) 500;
H. Meldner, Ark. Fys. 36 (1967) 593;
S.G. Nilsson, J.R. Nix, A. Sobiczewski, Z. Szymanski, S. Wycech, C. Gustafson, P. Möller, Nucl. Phys. A 115 (1968) 545;
U. Mosel, W. Greiner, Z. Phys. 222 (1969) 261;
E.O. Fiset, J.R. Nix, Nucl. Phys. A 193 (1972) 647;
J. Randrup, S.E. Larsson, P. Möller, S.G. Nilsson, K. Pomorski, A. Sobiczewski, Phys. Rev. C 13 (1976) 229;
P. Möller, J.R. Nix, J. Phys. G 20 (1994) 1681;
A. Sobiczewski, Phys. Part. Nucl. 25 (1994) 295;
R. Smolanczuk, J. Skalski, A. Sobiczewski, Phys. Rev. C 52 (1995) 1871;
I. Muntian, Z. Patyk, A. Sobiczewski, Phys. Rev. C 60 (1999) 041302.
[13] S. Cwiok, J. Dobaczewski, P.H. Heenen, P. Magierski, W. Nazarewicz, Nucl. Phys. A 611 (1996) 211;
K. Rutz, M. Bender, T. Bürvenich, T. Schilling, P.G. Reinhard, J.A. Maruhn, W. Greiner, Phys. Rev. C 56 (1997) 238;
A.T. Kruppa, M. Bender, W. Nazarewicz, P.-G. Reinhard, T. Vertse, S. Cwiok, Phys. Rev. C 61 (2000) 034313;
M. Bender, P.H. Heenen, P.G. Reinhard, Rev. Mod. Phys. 75 (2003) 121;
J. Meng, H. Toki, S.G. Zhou, S.Q. Zhang, W.H. Long, L.S. Geng, Prog. Part. Nucl. Phys. 57 (2006) 470.
[14] S. Hofmann, G. Münzenberg, Rev. Mod. Phys. 72 (2000) 733.

[15] Yu.Ts. Oganessian, Private communications (2015–2016).
[16] V.V. Volkov, Izv. Akad. Nauk SSSR, Ser. Fiz. 50 (1986) 1879;
N.V. Antonenko, E.A. Cherepanov, A.K. Nasirov, V.P. Permjakov, V.V. Volkov, Phys. Lett. B 319 (1993) 425;
Phys. Rev. C 51 (1995) 2635.
[17] G.G. Adamian, N.V. Antonenko, S.P. Ivanova, W. Scheid, Nucl. Phys. A 646 (1999) 29.
[18] G.G. Adamian, N.V. Antonenko, W. Scheid, V.V. Volkov, Nucl. Phys. A 633 (1998) 409;
Nuovo Cimento A 110 (1997) 1143.
[19] G.G. Adamian, N.V. Antonenko, W. Scheid, Nucl. Phys. A 678 (2000) 24.
[20] G.G. Giardina, S. Hofmann, A.I. Muminov, A.K. Nasirov, Eur. Phys. J. A 8 (2000) 205;
G.G. Giardina, F. Hanappe, A.I. Muminov, A.K. Nasirov, L. Stuttgé, Nucl. Phys. A 671 (2000) 165;
A.K. Nasirov, et al., Nucl. Phys. A 671 (2005) 342;
H.Q. Zhang, et al., Phys. Rev. C 81 (2010) 034611;
A.K. Nasirov, G. Mandaglio, G.G. Giardina, A. Sobiczewski, A.I. Muminov, Phys. Rev. C 84 (2011) 044612.
[21] Z.H. Liu, J.D. Bao, Phys. Rev. C 74 (2006) 057602.
[22] N. Wang, J. Tian, W. Scheid, Phys. Rev. C 84 (2011) 061601(R).
[23] N. Wang, E.G. Zhao, W. Scheid, S.G. Zhou, Phys. Rev. C 85 (2012) 041601(R);
N. Wang, E.G. Zhao, W. Scheid, Phys. Rev. C 89 (2014) 037601.
[24] L. Zhu, Z.Q. Feng, C. Li, F.S. Zhang, Phys. Rev. C 90 (2014) 014612;
Z.Q. Feng, G.M. Jin, J.Q. Li, W. Scheid, Phys. Rev. C 76 (2007) 044606.
[25] A.S. Zubov, G.G. Adamian, N.V. Antonenko, S.P. Ivanova, W. Scheid, Phys. Rev. C 68 (2003) 014616.
[26] G.G. Adamian, N.V. Antonenko, W. Scheid, A.S. Zubov, Phys. Rev. C 78 (2008) 044605.
[27] G.G. Adamian, N.V. Antonenko, W. Scheid, Clustering effects within the dinuclear model, in: Christian Beck (Ed.), Clusters in Nuclei, vol. 2, in: Lecture Notes in Physics, vol. 848, 2012, p. 165.
[28] J. Hong, G.G. Adamian, N.V. Antonenko, Phys. Rev. C 92 (2015) 014617.
[29] J. Hong, G.G. Adamian, N.V. Antonenko, Phys. Rev. C 94 (2016) 044606;
Eur. Phys. J. A 52 (2016) 305.
[30] V.S. Barashenkov, V.D. Toneev, High Energy Interaction of Particles and Nuclei with Atomic Nuclei, Atomizdat, Moscow, 1972.
[31] R. Vandenbosch, J.R. Huizenga, Nuclear Fission, Academic Press, New York, 1973.
[32] A. Ignatyuk, Statistical Properties of Excited Atomic Nuclei, Energoatomizdat, Moscow, 1983.
[33] E.A. Cherepanov, A.S. Iljinov, M.V. Mebel, J. Phys. G 9 (1983) 931.
[34] K.H. Schmidt, W. Morawek, Rep. Prog. Phys. 54 (1991) 949.
[35] A.S. Iljinov, et al., Nucl. Phys. A 543 (1992) 517.
[36] A.S. Zubov, G.G. Adamian, N.V. Antonenko, S.P. Ivanova, W. Scheid, Phys. Rev. C 65 (2002) 024308.
[37] S.G. Mashnik, A.J. Sierk, K.K. Gudima, arXiv:nucl-th/0208048, 2010.
[38] P. Möller, J.R. Nix, W.D. Myers, W.J. Swiatecki, At. Data Nucl. Data Tables 59 (1995) 185.
[39] G.G. Adamian, et al., Int. J. Mod. Phys. E 5 (1996) 191.